

Cite this: *Nanoscale*, 2023, 15, 11898

# LiCoO<sub>2</sub> cathode surface modification with optimally structured Li<sub>3</sub>PO<sub>4</sub> for outstanding high-voltage cycling performance†

Yuxuan Ji,<sup>a</sup> Jian Wei,<sup>\*a</sup> Di Liang,<sup>a</sup> Bing Chen,<sup>a</sup> Xueting Li,<sup>a</sup> Hao Zhang<sup>a</sup> and Zongyou Yin  <sup>\*b</sup>

While researchers often adopt a higher operating voltage to further enlarge the actual specific capacity of LCO to expand its application scope and market share, this triggers some more intractable issues in that the capacity decays obviously and causes the attendant problem of safety. Li<sub>3</sub>PO<sub>4</sub> shows the advantage of increasing the energy density of lithium-ion batteries due to its characteristic ionic conduction when coated onto an LCO cathode. Enhancing the conductivity of cathode materials is the key factor in the success of raising their operating voltage to meet emerging market demands. Here, we report a direct facile coprecipitation method for coating crystallized Li<sub>3</sub>PO<sub>4</sub> onto an LCO surface that enables balancing the ionic conductivity and chemical stability. LCO@Li<sub>3</sub>PO<sub>4</sub> crystalline lithium phosphate can generate superior electrical contact with the cathode material for high capacity and effectively stabilize the cathode surface by reducing the formation of SEI/CEI to prolong the cycle life. The optimized LP-3 cathode can deliver a high initial discharge capacity of 181 mA h g<sup>-1</sup> at 0.5C, with a capacity retention of 75% after 200 cycles. This study introduces a competitive strategy to produce a high-voltage LCO cathode *via* the most viable and economical method.

Received 18th March 2023,  
Accepted 23rd June 2023

DOI: 10.1039/d3nr01251d

rsc.li/nanoscale

## 1. Introduction

LCO has been the preferred choice for cathodes in recent decades due to its excellent layered structure, highest compaction density, attractive theoretical capacity (274 mA h g<sup>-1</sup>) and superb volumetric capacity (1363 mA h cm<sup>-3</sup>).<sup>1,2</sup> Unfortunately, when we constantly increase the cutoff charge voltage to obtain a higher specific capacity,<sup>3</sup> deep charging gives rise to the disappearance of the layered structure<sup>4</sup> and a series of negative side reactions, such as the corrosion of the cathode by HF, the dissolution of Co and the persistent generation of SEI/CEI,<sup>5</sup> leading to the rapid attenuation of capacity.<sup>6</sup> Hence, to ensure stable operation, the first applied voltage of commercial LCO is limited to 4.2 V, leading to a capacity of only up to half of the theoretical value.<sup>7</sup> It is urgent for us to further accelerate the research with regard to the stable operation of LCO at high voltage, which is the momentous basis for enhancing the competitiveness of LCO in the high-demand battery market.<sup>8</sup>

Various strategies have been explored to circumvent these drawbacks, such as elemental doping,<sup>9</sup> surface coating,<sup>10–12</sup> morphology design,<sup>13</sup> and employing separators,<sup>14</sup> electrolytes,<sup>15</sup> and the corresponding additives.<sup>16</sup> Although elemental doping shows a surprising result, the improvement is limited, especially at a higher voltage (>4.45 V) and under more extreme operating conditions. Doping is only effective in stabilizing the structure, eliminating the phase transition.<sup>4</sup> To date, no study has proven that doping can modify the surface structure to control surface reactions.<sup>17</sup> In this regard, surface coating is competitive in solving this intractable problem. The coating, just as an effective physical obstacle, impedes direct contact and hinders reactions between LCO and the electrolyte.<sup>18</sup> Researchers have explored, in recent years, all kinds of coating materials, including oxides,<sup>12,19–21</sup> fluorides,<sup>22–25</sup> and phosphates.<sup>26,27</sup> Owing to the superior strength of P=O bonds, phosphates have been regarded as a potential coating material to deliver higher electrochemical stability,<sup>17,28</sup> such as AlPO<sub>4</sub>,<sup>29</sup> FePO<sub>4</sub>,<sup>27</sup> Li<sub>3</sub>PO<sub>4</sub>,<sup>30</sup> LiCoPO<sub>4</sub>,<sup>49</sup> CePO<sub>4</sub>, and LiMgPO<sub>4</sub>.<sup>31</sup> Although they have outstanding electrochemical stability and improved cycle life, most of them introduce inactive elements, and their conductivity is poor,<sup>32</sup> which impedes ion and electron transfer, especially at high current densities.<sup>33</sup> On the other hand, other researchers have investigated, in recent years, fast ion conductor materials<sup>31,32,34,51</sup> and conductive

<sup>a</sup>College of Materials Science and Engineering, Xi'an University of Architecture and Technology, Xi'an 710055, China. E-mail: weijian@xauat.edu.cn

<sup>b</sup>Research School of Chemistry, The Australian National University, Canberra, Australian Capital Territory 2601, Australia. E-mail: zongyou.yin@anu.edu.au

† Electronic supplementary information (ESI) available. See DOI: <https://doi.org/10.1039/d3nr01251d>

polymers<sup>35,36</sup> to accelerate the transmission of ions or electrons, improving the electrochemical performance, such as PAN,<sup>36</sup> Li<sub>4</sub>Ti<sub>5</sub>O<sub>12</sub>,<sup>37</sup> LiVO<sub>2</sub>,<sup>32</sup> and Li<sub>2</sub>ZrO<sub>3</sub>.<sup>38</sup> Unfortunately, the cycling stability of most fast-ion conductor materials and conductive polymers is lower than that of phosphates.

Li<sub>3</sub>PO<sub>4</sub> is a representative choice, with higher ionic conductivity ( $\sim 6 \times 10^{-8}$  S cm<sup>-1</sup>) than most oxides or fluorides<sup>39</sup> while retaining the advantages of phosphates. For example, researchers have found that a slight coating of Li<sub>3</sub>PO<sub>4</sub> is favorable for enlarging the capacity of the cathode and increasing the redox electrochemical potentials, owing to the inductive effect of PO<sub>4</sub><sup>3-</sup> ions and reduced loss of Co<sup>3+</sup>.<sup>40</sup> Sun *et al.*<sup>41</sup> analyzed the mechanism by which a Li<sub>3</sub>PO<sub>4</sub> coating produced by a fire and quench method can improve the rate performance, as Li<sub>3</sub>PO<sub>4</sub> benefited the intercalation of Li<sup>+</sup>, thus leading to a better rate capacity than before. However, the coating formed by this method is not uniform enough. Zhou *et al.*<sup>30</sup> coated amorphous Li<sub>3</sub>PO<sub>4</sub> on LCO by magnetron sputtering, whether at room temperature (RT) or high temperature, and achieved outstanding cycling stability, which offers concrete support for the application potential of the Li<sub>3</sub>PO<sub>4</sub> coating. Y. Wang *et al.* developed a strategy through annealing a surface layer to form a high-voltage-stable surface coating layer *in situ*, which was demonstrated to be highly effective in improving the high-voltage performance of LiCoO<sub>2</sub>.<sup>48</sup> Although the coating formed by this method is more uniform, the preparation cost is high. Most researchers have found that crystalline coatings can achieve long stable cycling,<sup>32,37</sup> and for chemical stability, crystalline Li<sub>3</sub>PO<sub>4</sub> is superior to amorphous Li<sub>3</sub>PO<sub>4</sub>.<sup>33,42</sup> Therefore, the Li<sub>3</sub>PO<sub>4</sub> coating with a certain degree of crystallinity endows the electrode material with both good capacity and stability. Therefore, it is urgent to develop a more stable Li<sub>3</sub>PO<sub>4</sub> coating with a lower fabrication cost, which is more favorable for industrial applications.

In this paper, we used a scalable coprecipitation method with appropriate annealing, a mainly focused industrial method,<sup>43</sup> to develop phase tunable Li<sub>3</sub>PO<sub>4</sub> coating layers on the surface of LCO to prevent the deterioration of the cathode while accelerating the transmission of Li<sup>+</sup>. By further adjusting the annealing temperature and coating thickness, we found that LCO@Li<sub>3</sub>PO<sub>4</sub> can achieve an outstanding initial capacity of 181 mA h g<sup>-1</sup> with a retention of 90% after cycling at 0.5C and has a high reversible capacity of 132 mA h g<sup>-1</sup> at 3C, which is superior to many reported phosphates and fast ion conductor coatings, implying that using the wet chemical method to form the crystalline Li<sub>3</sub>PO<sub>4</sub> coating is a promising technique for the application of high-voltage LCO cathodes.

## 2. Experimental methods

### 2.1. Sample preparation

**2.1.1 Preparation of LCO@Li<sub>3</sub>PO<sub>4</sub>.** Bare LiCoO<sub>2</sub> powder (BLCO, Titan) was used as the pristine sample. LCO@Li<sub>3</sub>PO<sub>4</sub> (LP) was prepared by the coprecipitation method as follows: LiOH·H<sub>2</sub>O and NH<sub>4</sub>H<sub>2</sub>PO<sub>4</sub> were dissolved to obtain diluted

solutions A and B, respectively. LCO was added to solution A. After supersonic dispersion, the mixture was stirred for 12 h to facilitate the absorption of LCO to LiOH. Then, solution B was added to the uniform mixture and stirred at 80 °C. The black powder was annealed at 700 °C to prepare LP. We prepared four samples with different annealing times of 1, 3, 5 and 7 h, denoted as LP-1, LP-2, LP-3 and LP-4, respectively to explore the optimal preparation method and analyze the effect of the holding time.

### 2.2. Electrochemical tests

The mixing slurries were composed of active materials (LCO powder or LCO@LP powder, with a loading of 2.5–3 mg), polyvinylidene fluoride (PVDF), and acetylene black in a proportion of 8 : 1 : 1, cast on Al foil and dried at 120 °C for 6 h. Lithium was used as the anode, and Celgard 2500 was used as the separator to assemble CR2016 coin-type cells and then test the electrochemical properties. Charge–discharge tests were performed using the battery-testing system (LAND CT2001A); both LP electrodes and BLCO electrodes were conducted in the voltage range of 3–4.5 V at RT. The cycling performance was evaluated at current densities of 0.2, 0.5, 1, 2, and 3C (1C = 274 mA g<sup>-1</sup>). Electrochemical impedance spectroscopy (EIS) measurements in the frequency range of 10 mHz to 100 kHz and cyclic voltammetry (CV) tests in the potential range of 2.75 to 4.5 V were conducted on an electrochemical workstation (CHI660E, Donghua, China).

### 2.3. Characterization

We used scanning electron microscopy (FESEM, Gemini SEM 500) and transmission electron microscopy (TEM, FEI Talos F200X) to explore the structure and morphology of commercial LCO and LP particles, and the elemental distribution was identified by energy-dispersive spectrometry (EDS). The crystal structure was investigated by X-ray diffraction (XRD, X'Pert PRO), X-ray photoelectron spectra (XPS) were recorded using a Thermo ESCALAB 250XI, and Raman spectra were used to show the existence of the coating and the present state of PO<sub>4</sub><sup>3-</sup> at the surface.

### 2.4. Results and discussion

Fig. 1 (upper) shows the preparation procedure of LP. The hydrogen bond formed between the hydroxide and oxide results in LiOH to be absorbed on the surface of LiCoO<sub>2</sub> when stirred thoroughly. Then, NH<sub>4</sub>H<sub>2</sub>PO<sub>4</sub> reacts with LiOH to form Li<sub>3</sub>PO<sub>4</sub>, which thoroughly coats the surface. eqn (1) is used to confirm that no additional substances are generated.<sup>44,45</sup> The XRD patterns of the mixture of LiOH and NH<sub>4</sub>H<sub>2</sub>PO<sub>4</sub> after annealing are shown in Fig. S1,† where the phase of Li<sub>3</sub>PO<sub>4</sub> can be proven to exist, and excessive NH<sub>4</sub>H<sub>2</sub>PO<sub>4</sub> can ensure that LiOH, a substance harmful to capacity, can completely react as well as be beneficial for LP to show a cleaner surface than the uncoated one, which can also be confirmed from the XPS spectra.



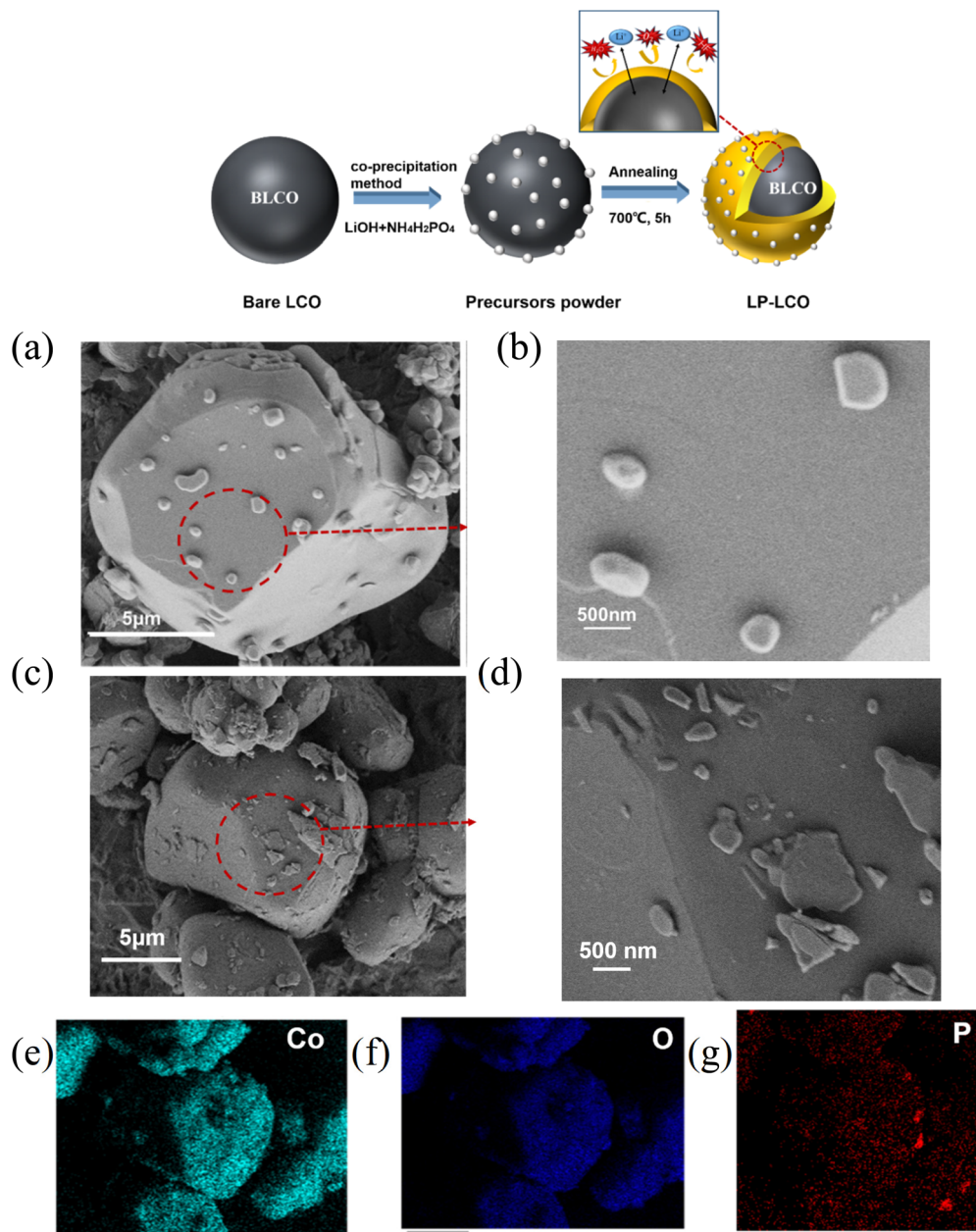


**Fig. 1** Top: schematic illustration of the preparation process of  $\text{Li}_3\text{PO}_4$  coated  $\text{LiCoO}_2$ . Bottom: (a and b) the SEM images of BLCO and (c and d) LP-3 and (e–g) the corresponding elemental maps.

In Fig. 1a–d, from the FESEM images, the particles of commercial LCO are irregular; the size is approximately 5–10 nm, and the surface is rough and porous, facilitating the formation of the coating. After coating, there are some unknown particles on the clean surface, and the difference in terms of the size and morphologies of the BLCO and LP powders is not obvious, demonstrating that the coating does not influence the main phase of the LCO. From the corresponding elemental maps of Co, O, and P in Fig. 1e–g, the coating obtained by the coprecipitation method is uniform. The images in Fig. S2† indicate that the size of  $\text{nanoLi}_3\text{PO}_4$  increased with the holding time.

The XRD patterns in Fig. 2a indicate that BLCO and all the LP electrodes exhibit the same peaks. This indicates that the  $\text{Li}_3\text{PO}_4$  coating does not influence the main phase and structure of bulk LCO, which is consistent with the conclusion from SEM, and the lack of additional peaks in accord with  $\text{Li}_3\text{PO}_4$  may be due to its comparatively low content or crystallinity.<sup>46</sup>

As the XRD results cannot directly confirm the existence of  $\text{Li}_3\text{PO}_4$ , Raman spectra and XPS spectra are used to explain the conditions of the BLCO and LP-3 surface. In Fig. 2b, after the coating, the spectra at  $481\text{ cm}^{-1}$  and  $592\text{ cm}^{-1}$  corresponding to the  $E_g$  (O–Co–O) and  $A_{1g}$  (Co–O) of LCO are not changed,

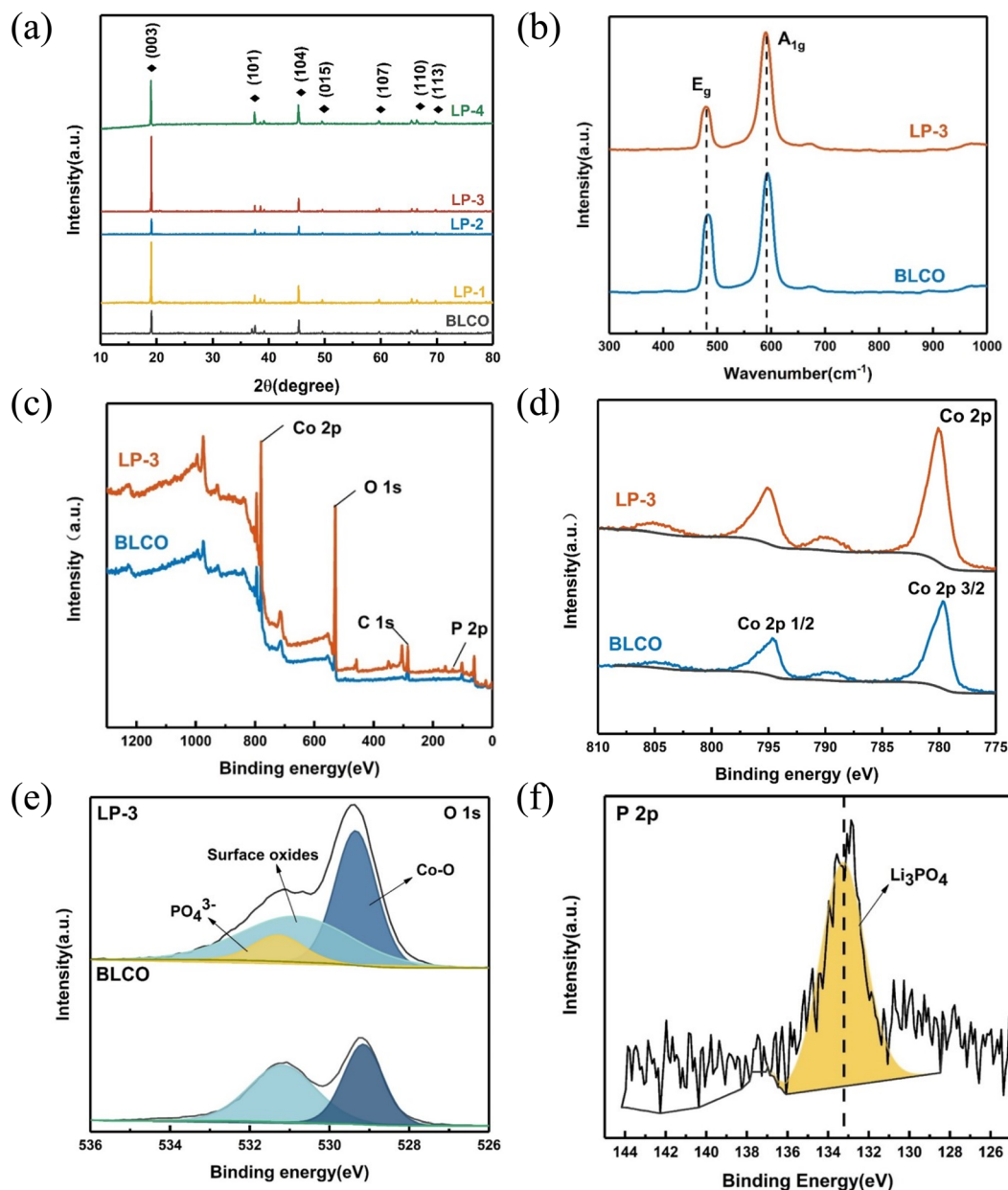


**Fig. 2** Phase analysis. (a) The XRD patterns of BLCO and LP, (b) the Raman spectra of BLCO and LP-3, and (c–f) the XPS spectra of BLCO and LP-3: (c) full spectra, (d and e) Co 2p and O 1s spectra of BLCO and LP-3, and (f) P 2p spectrum of LP-3.

and no additional peaks appear. This indicates that the main structure is still layered LCO, the coating is not doped in the layered structure, and the strength of the peaks is reduced, which also reflects some unknown substances on the surface. In Fig. 2c–f, the characteristic peak of P is only found in the LP-3 sample, from the full spectra in Fig. 2c, indicating that phosphorus does exist on the surface. Fig. 2d shows the Co 2p spectrum collected for LCO and LP-3. There are two main peaks in the spectra collected at Co 2p at nearly 795 eV and 780 eV for both samples corresponding to Co 2p<sub>1/2</sub> and Co 2p<sub>2/3</sub>, respectively,<sup>33</sup> which indicates that the coating does not influence the main components of LCO. Moreover, in the O 1s

spectra, it is notable that, after coating, we can find three kinds of characteristic peaks. The peak located at 529.34 eV corresponds to the slightly enhanced Co–O, which confirms that excessive NH<sub>4</sub>H<sub>2</sub>PO<sub>4</sub> can produce a cleaner surface, and the slightly minimized peak at 531.28 eV corresponds to the surface absorbed oxides,<sup>42</sup> indicating that some surface oxides may react with NH<sub>4</sub>H<sub>2</sub>PO<sub>4</sub> to form Li<sub>3</sub>PO<sub>4</sub>. In O 1s, we can find a new peak located at 530.84 eV, which represents PO<sub>4</sub><sup>3-</sup> on the surface. In the P 2p spectra, we see a distinct peak at 133.17 eV that can be ascribed to phosphate. The above evidence directly proves that Li<sub>3</sub>PO<sub>4</sub> was successfully coated on the LCO surface by this method.



To demonstrate the effect of different annealing times on the crystallinity of the coatings, the products with the shortest and longest annealing times, LP-1 and LP-3, were characterized by TEM. Enlarged LCO images and the corresponding FFT images are given in Fig. 3a–c, showing that the layered structure is still preserved well, with coatings on the surface. From the enlarged coating images (Fig. 3c), we can see the fuzzy lattice, and from the FFT images (Fig. 3e and h), it can be seen that the LP-3 coating is not amorphous, and the crystallinity is not high; it has slightly crystalline coating; However, in Fig. 3g and j, we cannot see the lattice and from the FFT images, we can conclude that the coating is amorphous. By comparison, it is clear that the longer the annealing time is, the higher the crystallinity of the coatings. In Fig. 3b and c, the  $\text{Li}_3\text{PO}_4$  coating is visible, with a thickness of approximately 20 nm. When  $\text{Li}_3\text{PO}_4$  is used as a coating material, higher crystallinity can reduce its ionic conductivity,<sup>47</sup> while certain crystallinity can resist the corrosion of  $\text{H}_2\text{O}$ ,  $\text{HF}$  and  $\text{O}_2$ ; low crystallinity causes  $\text{Li}_3\text{PO}_4$  to have certain ion conduction, accelerating the diffusion of  $\text{Li}^+$ ,<sup>47</sup> which can increase the initial

capacity while improving the cycle life. Consequently, we conclude that a  $\text{Li}_3\text{PO}_4$  coating layer with certain crystallinity could be achieved by changing the annealing conditions.<sup>48</sup>

In Fig. 4, we compared the electrochemical performance of BLCO and LP to study the effect of this modification and confirmed the optimal preparation method for  $\text{Li}_3\text{PO}_4$ , which is crucial to achieve the best cycling and rate performance of the cells. The initial discharge capacities (Fig. S3a†) of BLCO and LP at 0.1C are 184, 176, 171, 186 and 160  $\text{mA h g}^{-1}$ . The initial capacities of BLCO and LP are similar, indicating that the coating contributes little to the initial capacity, and improper crystallinity causes a large amount of highly crystalline  $\text{Li}_3\text{PO}_4$  to accumulate on the surface of LCO, which affects the transmission of electrons and reduces the initial capacity.

In Fig. 4a, we show the cycling performance of BLCO and LP and the values are listed in Table S1.† While the gap in the initial capacity is not obvious between BLCO and LP, the enhancement of cycling stability is noticeable for LP cathodes. The capacity of LCO decreased rapidly from 176.7 to 88.2  $\text{mA h g}^{-1}$  after 100 cycles. For LP cathodes, capacity retention was

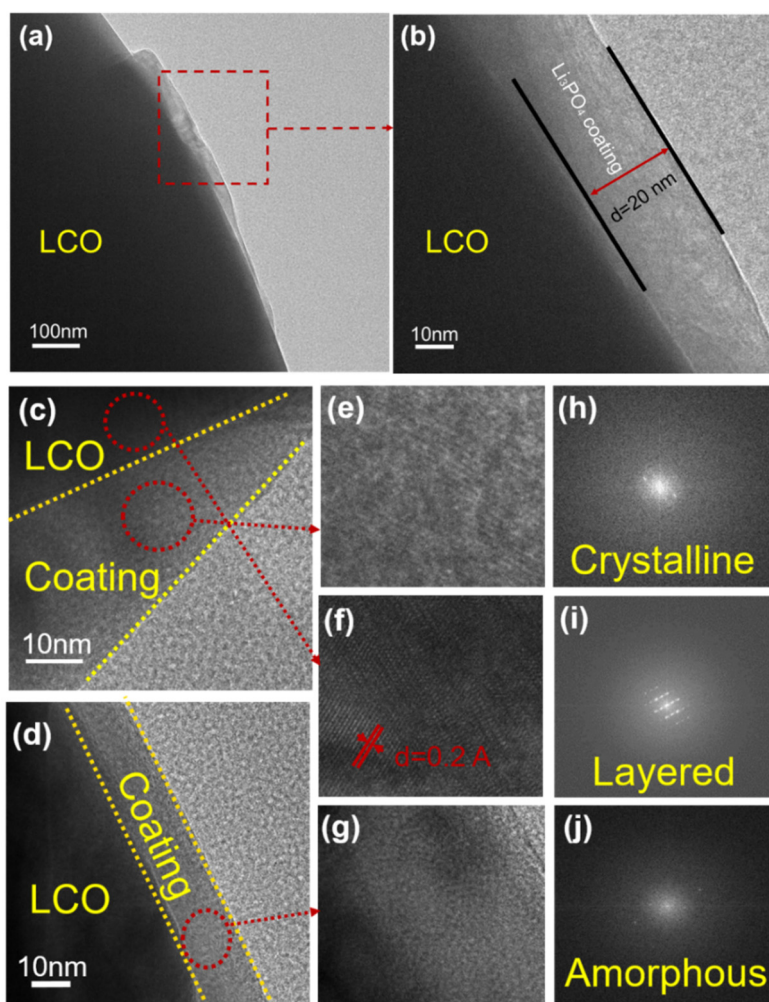
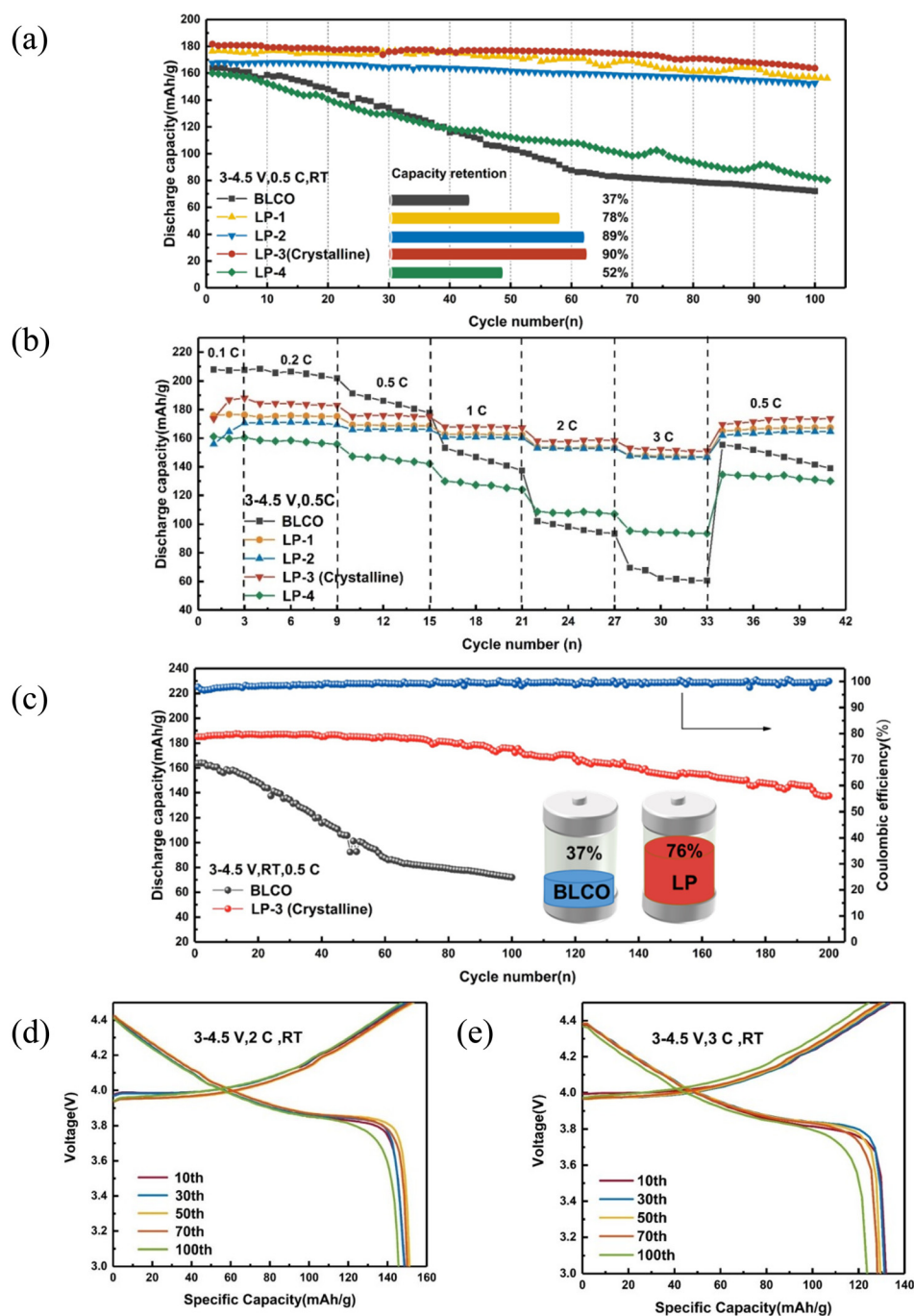


Fig. 3 TEM images of (a–c) LP-3 and (d) LP-1 and (e–j) enlarged images with the corresponding FFT images of LP-1 (g and j) and LP-3 (e, f and h–i).



**Fig. 4** The electrochemical performances of LP and BLCO cathodes. (a) The cycling performances and (b) the rate performances of BLCO and LP. (c) Long cycling performance. (d and e) The charge and discharge profiles of LP-3 at 2C and 3C, respectively.

78% (from 172 to 134 mA h g<sup>-1</sup>), 89% (from 168 to 152 mA h g<sup>-1</sup>), 90% (from 181 to 163 mA h g<sup>-1</sup>) and 52% (from 160 to 84 mA h g<sup>-1</sup>), while LCO lost half of its initial capacity from 176.7 to 88.2 mA h g<sup>-1</sup> after 100 cycles, indicating that proper crystallinity is beneficial for the cycling performance. Moreover, the outstanding ion conductivity can significantly alleviate the defect of the efficiency of low initial capacity by insulating coatings. The rate performances of BLCO and LP

are shown in Fig. 4b, and the values are listed in Table S2.† As the rate increased, for all the LP samples, the reversible capacity decreased slightly compared to that of BLCO. During the high rate of cycling, the capacity fading of LP-3 is obviously alleviated, with the highest reversible capacity reaching 152 mA h g<sup>-1</sup> at 3C. When the rate returns to 0.5C, the capacity retention of LP-3 is over 97%. All these results indicate that the Li<sub>3</sub>PO<sub>4</sub> coating can promote the transportation of Li<sup>+</sup> and

prevent the corrosion of electrolytes. In Fig. 4c, LP-3 maintained an ultrahigh capacity of  $137 \text{ mA h g}^{-1}$  after 200 cycles with a capacity retention of 76%. In Fig. 4d–e and Fig. S3c,† we show the cycling performance of LP-3 at 2C, 3C and 4C. After 100 cycles, the discharge platform is still well preserved, indicating that  $\text{Li}_3\text{PO}_4$  with proper crystallinity can protect the layered structure from the corrosion of the electrolyte during the cycling process. The capacity retention can

reach more than 90% after cycling at 2C and 3C. Moreover, the capacity can reach  $140 \text{ mA h g}^{-1}$  at 4C.

We show the CV of BLCO and LP-3 in Fig. S4a and b† to further explore the protective effect of the  $\text{Li}_3\text{PO}_4$  coating on the cathode structure. For the initial charge/discharge process, both BLCO and LP-3 show four reduction peaks,<sup>7</sup> and the most intense peak is at 3.81 V, which reflects the phase transitions between two hexagonal phases, H1 and H2. The oxi-

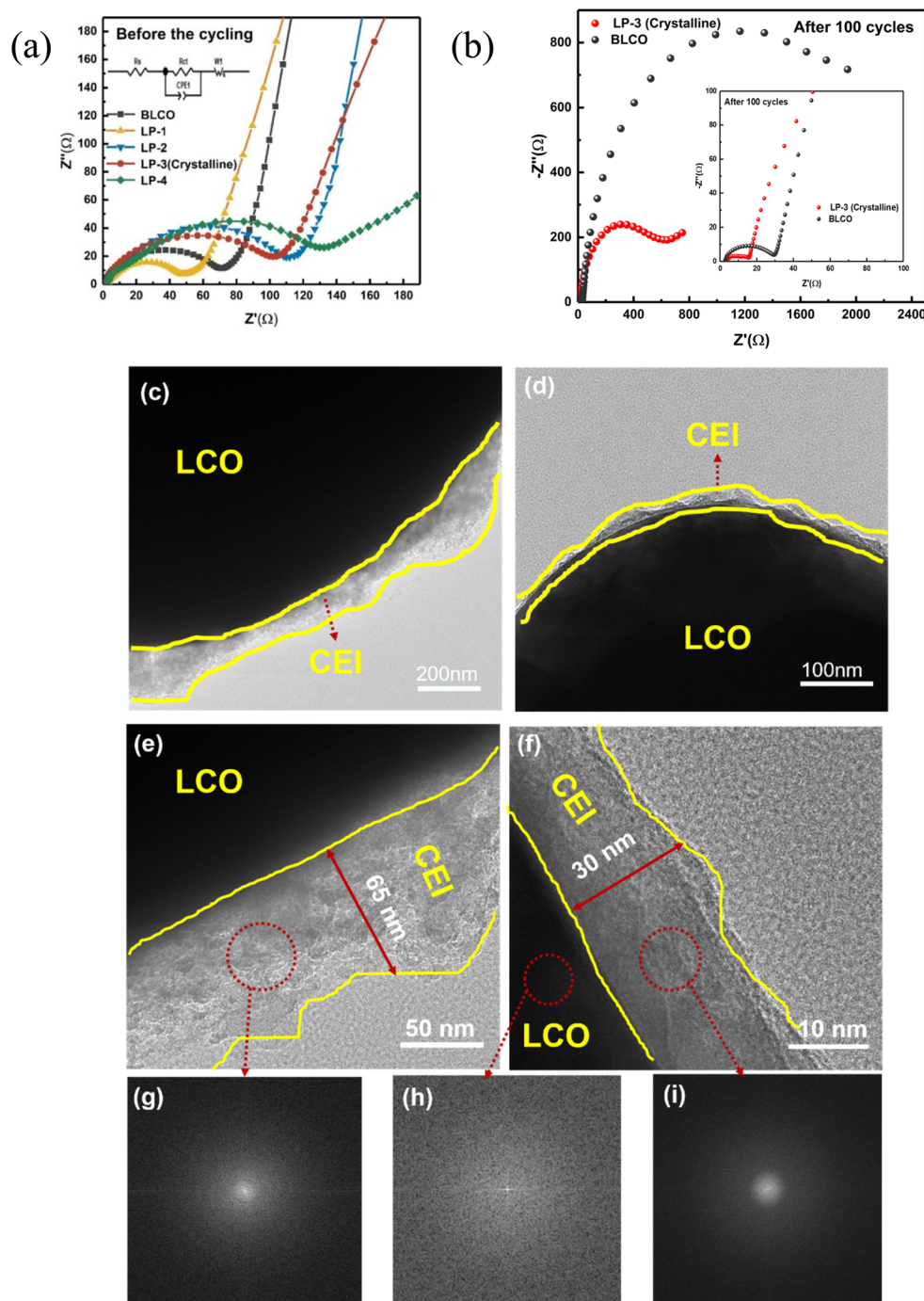


Fig. 5 Aging tests (a) EIS of BLCO and LP-3 before cycling and (b) EIS of BLCO and LP-3 after 100 cycles. TEM images of (c and e) BLCO and (d and f) LP-3 after 100 cycles and enlarged images with the corresponding FFT images (g–i).



ation peaks at 4.08 and 4.17 V are due to the order–disorder phase transitions.<sup>24</sup> After coating, the location of the redox peaks is not changed, and the strength is higher, which indicates that the reversible redox reactions that occur during the charging and discharging of the LCO cathodes are still present after coating, which enables the LCO to exhibit its optimal discharge capacity.

In Fig. 5a and b, we show the EIS profiles of BLCO and LP before and after the cycling test to explain the role of the  $\text{Li}_3\text{PO}_4$  coating, and after fitting, the specific value is shown in Table S3.† Crystalline  $\text{Li}_3\text{PO}_4$  is an insulating substance, while amorphous lithium phosphate has excellent ionic

conductivity.<sup>39,41</sup> Studies have shown that ionic conductive coatings can promote the transport of electrons and effectively improve the electrochemical properties of materials.<sup>48,50</sup> However, the amorphous lithium phosphate coating has poor stability, which is not conducive to the improvement of electrochemical stability. In terms of chemical stability, the crystalline  $\text{Li}_3\text{PO}_4$  is superior to the amorphous one.<sup>33</sup> The characteristics of lithium phosphate in different states influence the internal resistance. The resistance of LP-4, which has the highest crystallinity, is higher than that of any other sample. However, based on our subsequent electrochemical test results, low crystallinity has poor inert chemical properties.

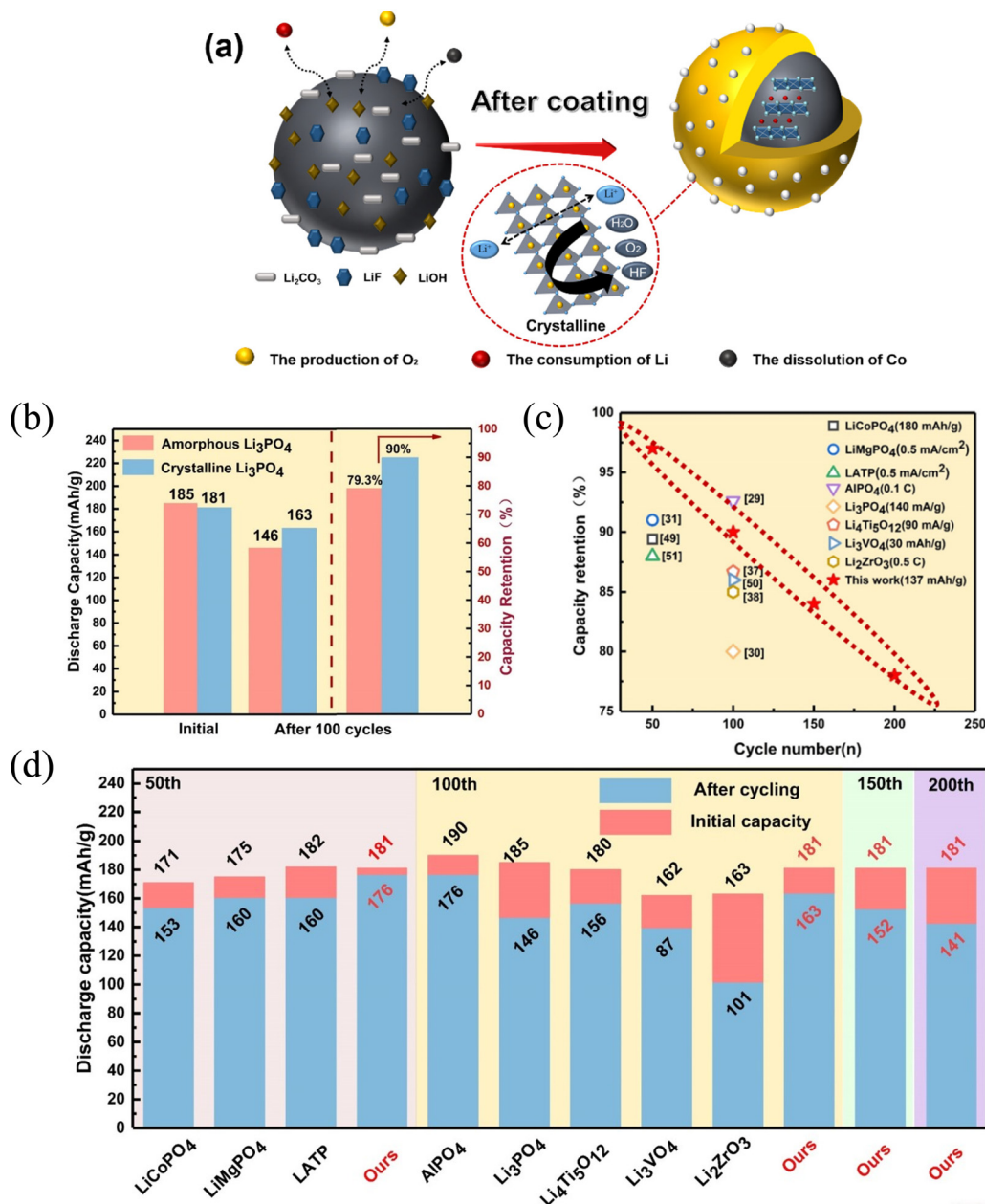


Fig. 6 (a) Schematic illustration of the crystalline  $\text{Li}_3\text{PO}_4$  coating effect, which can combine the advantages of chemical stability and ionic conductivity; comparison of (b) amorphous and crystalline  $\text{Li}_3\text{PO}_4$  coatings of LCO, (c and d) some phosphates and fast ion conductor coatings at the voltage of 4.5 V.



Therefore, we should explore a proper crystallinity that can balance the ionic conductivity and inert chemical properties, to achieve the best electrochemical performance.

To further demonstrate the protective effect of the coating, aging tests were carried out on LP-3, which has the best electrochemical properties. In Fig. 5a and b, after cycling, whether  $R_f$  or  $R_{ct}$ , the value of LP-3 is lower than that of BLCO, which indicates that the  $\text{Li}_3\text{PO}_4$  coating can stabilize the surface, reducing the formation of SEI/CEI and other substances that hamper the transfer of electric charge and increase the surface resistance. Fig. 5c–f show the TEM morphology of the BLCO and LP-3 electrodes after 100 cycles at 0.5C. Both of them generate an amorphous CEI film on the surface during the cycles, while the delicate film of LP-3 is thinner than that of BLCO. The enlarged images further disclose the surface situation of the two cycled cathodes. The part circled in yellow is the CEI film, which consists of harmful substances produced by the reaction between LCO and the electrolyte during the cycling process. The thickness of BLCO is over 65 nm and that of LP-3 is approximately 30 nm. The byproduct on LP-3 is thinner and more compact, which indicates that the coating effectively protects the cathode material and is not significantly different from the fresh cathode structure.

Based on previous analysis, we used the model in Fig. 6a to explain the role of the  $\text{Li}_3\text{PO}_4$  coating. It is well known that crystalline  $\text{Li}_3\text{PO}_4$  has a distinct structure with strong covalent bonding of P=O, which can maintain stability in HF,  $\text{O}_2$  and  $\text{H}_2\text{O}$ , allowing  $\text{Li}_3\text{PO}_4$  to act as a physical obstacle to mitigate the loss of  $\text{Co}^{3+}$  and suppress harmful side reactions, leading to outstanding cycling stability at high voltage.<sup>39</sup> Although amorphous  $\text{Li}_3\text{PO}_4$  is an outstanding ionic conductive material, it has less chemical inertness than crystalline  $\text{Li}_3\text{PO}_4$ , which dilutes its outstanding chemical inertness.<sup>42</sup> We used the coprecipitation method with the optimal annealing technique to form a coating, with certain crystallinity, to combine the advantages of both ion conductivity and inert chemical properties. It has superior inert chemical stability to most fast ion conductors. Simultaneously, as the crystallinity is not high,  $\text{Li}_3\text{PO}_4$  can possess better ion conductivity than most oxides and fluorides, accelerate  $\text{Li}^+$  diffusion and benefit the rate performance less than other oxides,<sup>47</sup> achieving the best balance between stability and transmission. Moreover, it does not introduce other additional metal elements, which is beneficial for reversible capacity. It is notable that this method is cheap and simple for mass production, which makes it more competitive in the high-voltage LCO market.

In Fig. 6b, we compare the initial capacity, capacity and retention after 100 cycles. We can see that the capacity and retention of crystalline  $\text{Li}_3\text{PO}_4$  are better than those of amorphous  $\text{Li}_3\text{PO}_4$ . Although certain crystallinity sacrifices a small amount of ionic conductivity and influences the initial capacity, it has better chemical stability, leading to higher capacity and retention after cycling. Table S4† lists some phosphates and fast ion conductor coatings. Different charge voltages and current densities provide obvious differences in capacity. Therefore, we chose some that worked at the cutoff voltage of 4.5 V and listed their different current densities to

compare the capacity retention and the specific capacity before and after the cycling, as shown in Fig. 6c and d. As  $\text{Li}_3\text{PO}_4$  with a certain crystallinity can combine the advantages of phosphates and fast ion conductor materials, it has higher chemical stability than some fast ion conductor materials and phosphates. By the wet chemical method, crystalline  $\text{Li}_3\text{PO}_4$  can be successfully coated on the LCO surface and a relatively superior electrochemical performance can be achieved.

## 2.5. Conclusion

In conclusion, a  $\text{Li}_3\text{PO}_4$  layer with certain crystallinity was successfully developed onto the LCO surface by the coprecipitation method (a kind of traditional wet chemical method). Compared with other insulating coatings, such as most oxides and fluorides, the  $\text{Li}_3\text{PO}_4$  coating is quite outstanding in terms of chemical stability and ionic conductivity; it protects the active material from corrosion by the electrolyte and facilitates the transportation of Li ions. LP-3 with proper crystalline coating delivers a capacity retention of 75% after 200 cycles, and it can deliver a higher capacity of 149 and 132  $\text{mA h g}^{-1}$  at 2C and 3C, respectively. In this work, we used a convenient method to achieve an ionic conductive coating with a certain degree of crystallinity to improve the cycling performance of LCO, and it can be a competitive candidate as the preparation technique for  $\text{LiCoO}_2$  coatings in high-voltage cycling performance lithium-ion batteries.

## Conflicts of interest

The authors declare that they have no known competing financial interests or personal relationships that could have appeared to influence the work reported in this paper.

## Acknowledgements

This project was supported by the National Natural Science Foundation of China (Grant No. 51578448, 51308447), the Natural Science Basic Research Plan in Shaanxi Province of China (Program No. 2017ZDJC18), the Scientific Research Program Funded by Shaanxi Provincial Education Department (Grant/Award No.: 20JY042) and the Technology Foundation for Selected Overseas Chinese Scholar, Ministry of Human Resources and Social Security of the People's Republic of China (Shan Ren She Han [2016]789).

## References

- 1 A. Holzer, S. Windisch-Kern, C. Ponak and H. Raupenstrauch, A Novel Pyrometallurgical Recycling Process for Lithium-Ion Batteries and Its Application to the Recycling of LCO and LFP, *Metals*, 2021, **11**, 149.
- 2 N. Nitta, F. Wu, J. T. Lee and G. Yushin, Li-ion battery materials: present and future, *Mater. Today*, 2015, **18**, 252–264.

- 3 X.-Q. Liao, F. Li, C.-M. Zhang, Z.-L. Yin, G.-C. Liu and J.-G. Yu, Improving the Stability of High-Voltage Lithium Cobalt Oxide with a Multifunctional Electrolyte Additive: Interfacial Analyses, *Nanomaterials*, 2021, **11**, 609.
- 4 J. Tan, Z. Wang, G. Li, H. Hu, J. Li, R. Han and D. Zhang, Electrochemically Driven Phase Transition in LiCoO<sub>2</sub> Cathode, *Materials*, 2021, **14**, 242.
- 5 W. Lu, J. Zhang, J. Xu, X. Wu and L. Chen, In Situ Visualized Cathode Electrolyte Interphase on LiCoO<sub>2</sub> in High Voltage Cycling, *ACS Appl. Mater. Interfaces*, 2017, **9**, 19313–19318.
- 6 Y. Jiang, C. Qin, P. Yan and M. Sui, Origins of capacity and voltage fading of LiCoO<sub>2</sub> upon high voltage cycling, *J. Mater. Chem. A*, 2019, **7**, 20824–20831.
- 7 K. Wang, J. J. Wan, Y. X. Xiang, J. P. Zhu, Q. Y. Leng, M. Wang, L. M. Xu and Y. Yang, Recent advances and historical developments of high voltage lithium cobalt oxide materials for rechargeable Li-ion batteries, *J. Power Sources*, 2020, **460**, 16.
- 8 J. B. Goodenough and K.-S. Park, The Li-Ion Rechargeable Battery: A Perspective, *J. Am. Chem. Soc.*, 2013, **135**, 1167–1176.
- 9 Q. Liu, X. Su, D. Lei, Y. Qin, J. Wen, F. Guo, Y. A. Wu, Y. Rong, R. Kou, X. Xiao, F. Aguesse, J. Bareno, Y. Ren, W. Lu and Y. Li, Approaching the capacity limit of lithium cobalt oxide in lithium ion batteries via lanthanum and aluminium doping, *Nat. Energy*, 2018, **3**, 936–943.
- 10 G. Lu, W. Peng, Y. Zhang, X. Wang, X. Shi, D. Song, H. Zhang and L. Zhang, Study on the formation, development and coating mechanism of new phases on interface in LiNbO<sub>3</sub>-coated LiCoO<sub>2</sub>, *Electrochim. Acta*, 2021, **368**, 137639.
- 11 N. H. Kwon, J. Conder, M. Srout and K. M. Fromm, Surface Modifications of Positive-Electrode Materials for Lithium Ion Batteries, *Chimia*, 2019, **73**, 880–893.
- 12 C. M. Julien, A. Mauger, H. Groult and K. Zaghib, Surface modification of positive electrode materials for lithium-ion batteries, *Thin Solid Films*, 2014, **572**, 200–207.
- 13 J. Ping, S. Rauf, Z. Tayyab, R. Wang, H. Xiao, L. Xu, S. Liang, Q. Huang and C. Yang, Effect of microstructure change on resistance of spherical LiCoO<sub>2</sub> to electrode degradation for proton intercalation, *Ceram. Int.*, 2021, **47**, 7898–7905.
- 14 S. C. Shin, J. Kim, J. K. R. Modigunta, G. Murali, S. Park, S. Lee, H. Lee, S. Y. Park and I. In, Bio-mimicking organic-inorganic hybrid ladder-like polysilsesquioxanes as a surface modifier for polyethylene separator in lithium-ion batteries, *J. Membr. Sci.*, 2021, **620**, 118886.
- 15 Z. Sun, H. Zhou, X. Luo, Y. Che, W. Li and M. Xu, Design of a novel electrolyte additive for high voltage LiCoO<sub>2</sub> cathode lithium-ion batteries: Lithium 4-benzonitrile trimethyl borate, *J. Power Sources*, 2021, **503**, 230033.
- 16 L. Sheng, L. Song, H. Gong, J. Pan, Y. Bai, S. Song, G. Liu, T. Wang, X. Huang and J. He, Polyethylene separator grafting with polar monomer for enhancing the lithium-ion transport property, *J. Power Sources*, 2020, **479**, 228812.
- 17 L. Wang, B. Chen, J. Ma, G. Cui and L. Chen, Reviving lithium cobalt oxide-based lithium secondary batteries-toward a higher energy density, *Chem. Soc. Rev.*, 2018, **47**, 6505–6602.
- 18 S.-W. Lee, M.-S. Kim, J. H. Jeong, D.-H. Kim, K. Y. Chung, K. C. Roh and K.-B. Kim, Li<sub>3</sub>PO<sub>4</sub> surface coating on Ni-rich LiNi<sub>0.6</sub>Co<sub>0.2</sub>Mn<sub>0.2</sub>O<sub>2</sub> by a citric acid assisted sol-gel method: Improved thermal stability and high-voltage performance, *J. Power Sources*, 2017, **360**, 206–214.
- 19 A. Zhou, Q. Liu, Y. Wang, W. Wang, X. Yao, W. Hu, L. Zhang, X. Yu, J. Li and H. Li, Al<sub>2</sub>O<sub>3</sub> surface coating on LiCoO<sub>2</sub> through a facile and scalable wet-chemical method towards high-energy cathode materials withstanding high cutoff voltages, *J. Mater. Chem. A*, 2017, **5**, 24361–24370.
- 20 A. Zhou, W. Wang, Q. Liu, Y. Wang, X. Yao, F. Qing, E. Li, T. Yang, L. Zhang and J. Li, Stable, fast and high-energy-density LiCoO<sub>2</sub> cathode at high operation voltage enabled by glassy B<sub>2</sub>O<sub>3</sub> modification, *J. Power Sources*, 2017, **362**, 131–139.
- 21 S. Pavithra, P. Arjunan, M. Jayachandran, R. Kalaivani, M. Selvapandiyan and N. Sivakumar, Investigations on electrochemical performance of the full cell fabricated LiCoO<sub>2</sub> wrapped with MgO and ZnO for advanced lithium ion battery applications, *J. Mater. Sci.: Mater. Electron.*, 2020, **31**, 15505–15512.
- 22 Z. Yang, Q. Qiao and W. Yang, Improvement of structural and electrochemical properties of commercial LiCoO<sub>2</sub> by coating with LaF<sub>3</sub>, *Electrochim. Acta*, 2011, **56**, 4791–4796.
- 23 H. J. Lee and Y. J. Park, Interface characterization of MgF<sub>2</sub>-coated LiCoO<sub>2</sub> thin films, *Solid State Ionics*, 2013, **230**, 86–91.
- 24 Y. Bai, K. Jiang, S. Sun, Q. Wu, X. Lu and N. Wan, Performance improvement of LiCoO<sub>2</sub> by MgF<sub>2</sub> surface modification and mechanism exploration, *Electrochim. Acta*, 2014, **134**, 347–354.
- 25 J. S. Park, A. U. Mane, J. W. Elam and J. R. Croy, Atomic Layer Deposition of Al-W-Fluoride on LiCoO<sub>2</sub> Cathodes: Comparison of Particle-and Electrode-Level Coatings, *ACS Omega*, 2017, **2**, 3724–3729.
- 26 E. Jung and Y. J. Park, Characterization of thermally aged AlPO<sub>4</sub>-coated LiCoO<sub>2</sub> thin films, *Nanoscale Res. Lett.*, 2012, **7**, 1–4.
- 27 K. C. Kim, J.-P. Jegal, S.-M. Bak, K. C. Roh and K.-B. Kim, Improved high-voltage performance of FePO<sub>4</sub>-coated LiCoO<sub>2</sub> by microwave-assisted hydrothermal method, *Electrochem. Commun.*, 2014, **43**, 113–116.
- 28 J. Niu, M. Wang, T. Cao, X. Cheng, R. Wu, H. Liu, Y. Zhang and X. Liu, Li metal coated with Li<sub>3</sub>PO<sub>4</sub> film via atomic layer deposition as battery anode, *Ionics*, 2021, **27**, 2445–2454.
- 29 F. L. Yang, W. Zhang, Z. X. Chi, F. Q. Cheng, J. T. Chen, A. M. Cao and L. J. Wan, Controlled formation of core-shell structures with uniform AlPO<sub>4</sub> nanoshells, *Chem. Commun.*, 2015, **51**, 2943–2945.
- 30 A. Zhou, J. Xu, X. Dai, B. Yang, Y. Lu, L. Wang, C. Fan and J. Li, Improved high-voltage and high-temperature electro-

- chemical performances of LiCoO<sub>2</sub> cathode by electrode sputter-coating with Li<sub>3</sub>PO<sub>4</sub>, *J. Power Sources*, 2016, **322**, 10–16.
- 31 H. Morimoto, H. Awano, J. Terashima, S. Nakanishi, Y. Hiram, K. Ishikawa and S.-i. Tobishima, Charge-discharge properties of LiCoO<sub>2</sub> electrodes modified by olivine-type compounds of LiMgPO<sub>4</sub> for lithium secondary batteries, *J. Power Sources*, 2012, **211**, 66–70.
- 32 X. Pu, L. Yin and C. Yu, Functional surface modifications on nanostructured LiCoO<sub>2</sub> with lithium vanadates, *J. Nanopart. Res.*, 2012, **14**, 788.
- 33 P. Zou, Z. Lin, M. Fan, F. Wang, Y. Liu and X. Xiong, Facile and efficient fabrication of Li<sub>3</sub>PO<sub>4</sub>-coated Ni-rich cathode for high-performance lithium-ion battery, *Appl. Surf. Sci.*, 2020, **504**, 144506.
- 34 Y. Kim, G. M. Veith, J. Nanda, R. R. Unocic, M. Chi and N. J. Dudney, High voltage stability of LiCoO<sub>2</sub> particles with a nano-scale Lipon coating, *Electrochim. Acta*, 2011, **56**, 6573–6580.
- 35 J. Cao, G. Hu, Z. Peng, K. Du and Y. Cao, Polypyrrole-coated LiCoO<sub>2</sub> nanocomposite with enhanced electrochemical properties at high voltage for lithium-ion batteries, *J. Power Sources*, 2015, **281**, 49–55.
- 36 X. Yang, L. Shen, B. Wu, Z. Zuo, D. Mu, B. Wu and H. Zhou, Improvement of the cycling performance of LiCoO<sub>2</sub> with assistance of cross-linked PAN for lithium ion batteries, *J. Alloys Compd.*, 2015, **639**, 458–464.
- 37 C.-W. Wang, Y. Zhou, J.-H. You, J.-D. Chen, Z. Zhang, S.-J. Zhang, C.-G. Shi, W.-D. Zhang, M.-H. Zou, Y. Yu, J.-T. Li, L.-Y. Zeng, L. Huang and S.-G. Sun, High-Voltage LiCoO<sub>2</sub> Material Encapsulated in a Li<sub>(4)</sub>Ti<sub>(5)</sub>O<sub>(12)</sub> Ultrathin Layer by High-Speed Solid-Phase Coating Process, *ACS Appl. Energy Mater.*, 2020, **3**, 2593–2603.
- 38 J. C. Zhang, R. Gao, L. M. Sun, H. Zhang, Z. B. Hu and X. F. Liu, Unraveling the multiple effects of Li<sub>2</sub>ZrO<sub>3</sub> coating on the structural and electrochemical performances of LiCoO<sub>2</sub> as high-voltage cathode materials, *Electrochim. Acta*, 2016, **209**, 102–110.
- 39 C.-H. Jo, D.-H. Cho, H.-J. Noh, H. Yashiro, Y.-K. Sun and S. T. Myung, An effective method to reduce residual lithium compounds on Ni-rich Li Ni<sub>0.6</sub>Co<sub>0.2</sub>Mn<sub>0.2</sub>O<sub>2</sub> active material using a phosphoric acid derived Li<sub>3</sub>PO<sub>4</sub> nanolayer, *Nano Res.*, 2015, **8**, 1464–1479.
- 40 M. Sawamura, S. Kobayakawa, J. Kikkawa, N. Sharma, D. Goonetilleke, A. Rawal, N. Shimada, K. Yamamoto, R. Yamamoto, Y. Zhou, Y. Uchimoto, K. Nakanishi, K. Mitsuhashi, K. Ohara, J. Park, H. R. Byon, H. Koga, M. Okoshi, T. Ohta and N. Yabuuchi, Nanostructured LiMnO<sub>2</sub> with Li<sub>3</sub>PO<sub>4</sub> Integrated at the Atomic Scale for High-Energy Electrode Materials with Reversible Anionic Redox, *ACS Cent. Sci.*, 2020, **6**, 2326–2338.
- 41 K. Sun and S. J. Dillon, A mechanism for the improved rate capability of cathodes by lithium phosphate surficial films, *Electrochem. Commun.*, 2011, **13**, 200–202.
- 42 Y. Su, F. Yuan, L. Chen, Y. Lu, J. Dong, Y. Fang, S. Chen and F. Wu, Enhanced high-temperature performance of Li-rich layered oxide via surface heterophase coating, *J. Energy Chem.*, 2020, **51**, 39–47.
- 43 X. Tan, M. Zhang, J. Li, D. Zhang, Y. Yan and Z. Li, Recent progress in coatings and methods of Ni-rich LiNi<sub>0.8</sub>Co<sub>0.1</sub>Mn<sub>0.1</sub>O<sub>2</sub> cathode materials: A short review, *Ceram. Int.*, 2020, **46**, 21888–21901.
- 44 X. Bian, Q. Fu, X. Bie, P. Yang, H. Qiu, Q. Pang, G. Chen, F. Du and Y. Wei, Improved Electrochemical Performance and Thermal Stability of Li-excess Li<sub>1.18</sub>Co<sub>0.15</sub>Ni<sub>0.15</sub>Mn<sub>0.52</sub>O<sub>2</sub> Cathode Material by Li<sub>3</sub>PO<sub>4</sub> Surface Coating, *Electrochim. Acta*, 2015, **174**, 875–884.
- 45 J.-N. Zhang, Q. Li, Y. Wang, J. Zheng, X. Yu and H. Li, Dynamic evolution of cathode electrolyte interphase (CEI) on high voltage LiCoO<sub>2</sub> cathode and its interaction with Li anode, *Energy Storage Mater.*, 2018, **14**, 1–7.
- 46 S. He, A. Wei, W. Li, X. Bai, L. Zhang, L. Yang and Z. Liu, Al-Ti-oxide coated LiCoO<sub>2</sub> cathode material with enhanced electrochemical performance at a high cutoff charge potential of 4.5 V, *J. Alloys Compd.*, 2019, **799**, 137–146.
- 47 L. Wang, Q. Wang, W. Jia, S. Chen, P. Gao and J. Li, Li metal coated with amorphous Li<sub>3</sub>PO<sub>4</sub> via magnetron sputtering for stable and long-cycle life lithium metal batteries, *J. Power Sources*, 2017, **342**, 175–182.
- 48 Y. Wang, Q. Wu, S. Li, Z. Tong, D. Wang, H. L. Zhuang, Y. Wang and Y. Lu, Lithium-Aluminum-Phosphate coating enables stable 4.6 V cycling performance of LiCoO<sub>2</sub> at room temperature and beyond, *Energy Storage Mater.*, 2021, **37**, 67–76.
- 49 H. Lee, M. G. Kim and J. Cho, Olivine LiCoPO<sub>4</sub> phase grown LiCoO<sub>2</sub> cathode material for high density Li batteries, *Electrochem. Commun.*, 2006, **9**, 149–154.
- 50 X. Pu and C. Yu, Enhanced overcharge performance of nano-LiCoO<sub>2</sub> by novel Li<sub>3</sub>VO<sub>4</sub> surface coatings, *Nanoscale*, 2012, **4**, 6743–6747.
- 51 H. Morimoto, H. Awano, J. Terashima, Y. Shindo, S. Nakanishi, N. Ito, K. Ishikawa and S. Tobishima, Preparation of lithium ion conducting solid electrolyte of NASICON-type Li<sub>1+x</sub>Al<sub>x</sub>Ti<sub>2-x</sub>(PO<sub>4</sub>)<sub>3</sub> (x = 0.3) obtained by using the mechanochemical method and its application as surface modification materials of LiCoO<sub>2</sub> cathode for lithium cell, *J. Power Sources*, 2013, **240**, 636–643.